Article

Human Adipose Stem Cell-derived Extracellular Vesicles Induce Immune Responses in Mice but Not in Human Peripheral Blood Mononuclear Cells

Dong Oh Kim [1,2], Young Chan Choi [3], Woojin Kim [1], Ji Suk Choi [3], Kyoung Soo Lee [3], Yong Woo Cho [3,4], Byoung-Seok Lee [1,*] and Min Heui Yoo [1,*]

[1] Department of Innovative Toxicology Research, Korea Institute of Toxicology, 141 Gajeon-ro, Yuseong-gu, Daejeon, Republic of Korea; minheui.yoo@kitox.re.kr (M.H.Y.); do.kim@sc-bio.co.kr (D.O.K.); woojinkim@kitox.re.kr (W.K.); bslee@kitox.re.kr (B.-S.L.)
[2] R&D Center, SCBIO Co, Ltd, 94-14 Techno 2-ro, Yuseong-gu, Daejeon, Republic of Korea; do.kim@sc-bio.co.kr (D.O.K.)
[3] ExoStemTech, Inc., Ansan, Gyeonggi-do, Republic of Korea; ycchoi@exostemtech.com (Y.C.C.); jschoi@exostemtech.com (J.S.C.); kslee@exostemtech.com (K.S.L.); ywcho7@hanyang.ac.kr (Y.W.C.)
[4] Department of Materials Science and Chemical Engineering, Hanyang University ERICA, Ansan, Gyeonggi-do, Republic of Korea; ywcho7@hanyang.ac.kr (Y.W.C.)
* Correspondence: minheui.yoo@kitox.re.kr (M.H.Y.); bslee@kitox.re.kr (B.-S.L.); Tel.: +82-42-610-8424

Abstract: Human adipose stem cell-derived extracellular vesicles (hASC-EVs) are key mediators of paracrine signaling with promising therapeutic applications. Although hASC-EVs are derived from human cells and are less immunogenic, their immunogenicity cannot be completely excluded. Here, we evaluate the immune responses of ICR and C57BL/6 mice to high doses of hASC-EVs for 10 days after injection. Lymphocyte subpopulations are analyzed using flow cytometry at 0.5, 1, 3 and 24 h post injection. In the spleen and blood of C57BL/6 mice, neutrophils sharply increased at 0.5 h and decreased at 3 h following hASC-EV treatment. We observe increased proportions of monocytes, macrophages, and natural killer cells at 3 h but returned to similar level of vehicle control at 24 h post injection in the spleen and blood of ICR mice. Although the in vivo experiments reveal different immune responses to hASC-EV treatment in C57BL/6 and ICR strains, no major changes occur in human peripheral blood mononuclear cell composition after applying hASC-EVs in vitro. In conclusion, unlike those in mice, immune responses to hASC-EVs in humans are not detectable, indicating a minimal risk of fatal side-effects from hASC-EV-based therapies.

Keywords: human adipose mesenchymal stem cells; human peripheral blood mononuclear cells; immune cell frequencies; C57BL/6 mice; ICR mice

1. Introduction

Depending on their size, extracellular vesicles (EVs) are defined as microvesicles (MVs) or exosomes. MVs are 150–1000 nm in size and are formed by direct outward budding from the cell membrane. Exosomes are 50–200 nm in size and are mainly released from multivesicular bodies fusing with the plasma membrane. In this study, we used two different mouse strains and human peripheral blood mononuclear cells (hPBMCs) to confirm the non-clinical immunotoxicity of exosomes produced from human adipose-derived mesenchymal stem cells (MSCs).

Human MSCs have been proposed as therapeutic agents for various diseases, including graft-versus-host disease [1] and cardiac [2], neurological [3], and orthopedic disorders [4]. However, the limitations of MSCs such as their tumorigenic potential and storage difficulties necessitate the search for treatment alternatives. Emerging evidence indicates that EVs are among the most promising substitutes for cell therapy. For example, MSC-derived EVs contain various growth factors, cytokines, and microRNAs (from the

Preprints (www.preprints.org) | NOT PEER-REVIEWED | Posted: 5 December 2022 doi:10.20944/preprints202212.0069.v1

parental MSCs) and thus possess the advantages of stem cells. In contrast to cells, EVs cannot divide, and tumorigenesis can be ruled out [5]. EVs play essential roles in remodeling the extracellular matrix and transmitting information between cells [6]. However, one of the limitations of EVs as therapeutics is their effect on the human immune system. Since EVs contain multiple proteins, RNAs, microRNAs, and cytokines inherited from the cell of origin [7], it is not difficult to predict the complex interactions between EVs and human immunity. Therefore, preclinical studies are required to determine how therapeutic EVs may affect the immune system in humans.

EVs can activate or suppress the immune system [8,9]. These opposing effects are determined by the cell type that EVs originate from. EVs can modulate the immune responses bidirectionally according to the experimental data obtained using *in vitro* and *in vivo* models. Tumor-derived EVs can positively affect anti-cancer immune responses by activating immune cells. Leukemia cell-derived EVs induce the secretion of interleukin (IL)-12p70 and tumor necrosis factor (TNF)-α to promote dendritic cell function [10]. Such vesicles contain high levels of heat shock protein (HSP) 90 and immunogenic molecules (such as major histocompatibility complex [MHC] I, MHC II, cluster of differentiation [CD] 40, CD86, regulated on activation, normal T cell expressed and secreted [RANTES], and IL-1β), thereby enabling the effective activation of $CD8^+$ T cells and eliciting an antitumor effect [10]. MSC-derived exosomes can alleviate inflammatory damages induced by sepsis by reprogramming the metabolism of macrophages [11,12]. MSC-derived exosomes induced regulatory T (Treg) cell expansion by inducing an anti-inflammatory M2-like phenotype in monocytes [13,14]. Epithelial cell-derived EVs can affect the immune system. The effect of lung epithelial-derived exosomes on macrophages during sepsis is mainly characterized by immune activation and the induction of inflammation. Hyperoxia-induced, lung epithelial-derived, and caspase-3-enriched EVs (including exosomes) activate macrophages via the ROCK1 pathway and increase the secretion of pro-inflammatory cytokines and macrophage inflammatory protein 2 (MIP-2) [15]. Exosomes from intestinal epithelial cells contain pro-inflammatory cytokines, which promote the migration of macrophages and exacerbate the inflammatory response [16].

Ample data indicate that EVs can induce immunosuppression. In one study, exosomes extracted from B16F10 melanoma cells were shown to suppress cytotoxic immunity by altering the transcriptome of cytotoxic T lymphocytes (CTLs) such that mitochondrial respiration does not depend on hypoxia [17]. Another report showed that exosomes secreted from MSCs upregulated the expression of IL-10 and transforming growth factor (TGF)-β1 in PBMCs, thereby suppressing Treg proliferation in patients with asthma [18]. EVs containing the tumor antigen ovalbumin (OVA) suppressed the delayed-type hypersensitivity response to OVA [19]. Tumor-derived EVs are acquired by endogenous antigen presenting cells that suppress immune responses after plantar OVA injection. In addition, tumor-derived EVs inhibited the differentiation of $CD11b^+$ precursor cells in the bone marrow *in vivo* and induced IL-6 expression in immune cells [20,21].

Therefore, the effects of cell-derived EVs on the immune system depend on the parental cell type, and their immunotoxicity and immunogenicity cannot be completely understood without pre-clinical research. In this study, we investigated the influence of human adipose stem cell-derived extracellular vesicles (hASC-EVs; currently being developed as an anti-inflammatory treatment) on the immune system, via both *in vivo* and *in vitro* approaches, using flow cytometry.

2. Results

2.1. Study Design and Changes in the Total Number of Cells in the Spleens of C57BL/6 and ICR Mice After hASC-EV Administration

hASC-EVs were administered to C57BL/6 and ICR mice according to the experimental pipeline shown in Figure 1a. After one week of acclimatization, the

Preprints (www.preprints.org) | NOT PEER-REVIEWED | Posted: 5 December 2022 doi:10.20944/preprints202212.0069.v1

experiment was started by dividing the acclimatized mice into groups. The mice were treated intravenously with 1 × 10^9 hASC-EV particles or the same volume of PBS five times over 10 days. At 0.5, 1, and 3 h after the last treatment, the mice were sacrificed by overdosing with isoflurane, and blood and spleens were collected. Changes in the relative abundances of immune cells in the blood and spleen samples were analyzed using a CytoFLEX flow cytometer (Figure 1a). Analysis using a Vi-Cell® XR Cell Viability Analyzer (Beckman Coulter, High Wycombe, UK) confirmed that the number of cells in the spleen tissues increased significantly in the group that received hASC-EVs, at 1 h after administration (Figure 1b). Similar increases were observed in both C57BL/6 and ICR mice. Specifically, similar patterns showing increased cell numbers were observed in the spleens of both mice within 1 h following intravenous administration of hASC-EVs. At 3 h post- administration, the number of cells was similar to that in the vehicle-administered group.

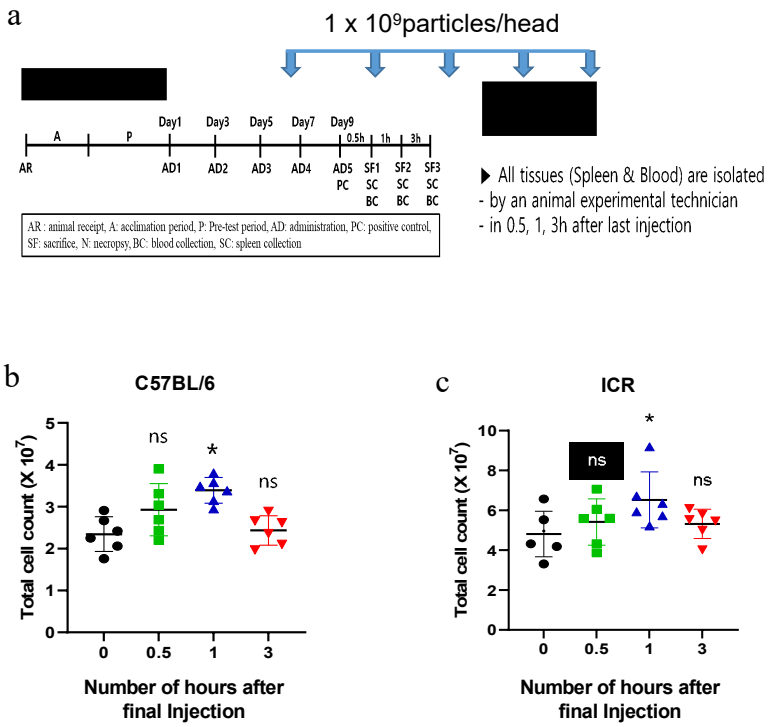

Figure 1. Study design and changes in total cell count in the spleens of C57BL/6 and ICR mice after hASC-EV administration. **(a)** Animal study designed to test immune responses to hASC-EVs in C57BL/6 and ICR mice. After administering hASC-EVs five times over 10 days, spleen and blood samples were harvested to analyze immune cell changes at 0.5, 1, and 3 h after the last injection. **(b)** Analysis of splenocyte changes in the spleens of both mouse strains after five hASC-EV administrations. One hour after administration, a significant increase in the total splenocytes is observed in both C57BL/6 and ICR mice (n = 5–6 mice; one-way ANOVA, *$p < 0.05$). *ns:* not significant.

2.2. Analysis of Immune Cell Frequency in the Spleens and Blood of C57BL/6 Mice at Short-term Time Points After Administrating hASC-EVs Five Times

After administering hASC-EVs intravenously to C57BL/6 mice, the suspensions of spleen cells were incubated with immune cell-specific antibodies and the frequencies of immune cells were analyzed by flow cytometry. Macrophage markers (CD14 and CD1b antibodies) were detected to confirm the frequency of macrophages in the spleen. According to the results, no significant increase in macrophage numbers was observed at 0.5 h after hASC-EV administration, although significant decreases were observed at 1 and 3 h after administration (Figure 2a). We observed a significant increase in neutrophil numbers at 0.5 h after hASC-EV administration, but they returned to baseline levels (0 h

Preprints (www.preprints.org) | NOT PEER-REVIEWED | Posted: 5 December 2022 doi:10.20944/preprints202212.0069.v1

after vehicle administration) by 1 and 3 h after hASC-EV administration. B cell splenocyte levels were significantly lower at 0.5 h post administration but reached normal levels subsequently. No change in the frequency of dendritic cells was observed following hASC-EV administration (Figure 2a). A significant decrease was observed in natural killer (NK) cell numbers at 1 and 2 h after hASC-EV administration, whereas no significant changes in T cell levels were observed at any time point (Figure 2a). We also performed immune cell analysis with blood samples taken from C57BL/6 mice after hASC-EV administration. The frequency of neutrophils in the blood significantly increased at 0.5 h after hASC-EV administration, similar to that observed in the spleen, and then decreased over time. The macrophage levels in the blood changed substantially after hASC-EV administration, although the levels of B cells and dendritic cells significantly decreased at 0.5 h post administration and then recovered over time (Figure 2b). In contrast to the results obtained with spleen samples, the levels of NK cells, total T cells, CTLs, and T-helper cells decreased significantly at 0.5 h after hASC-EV administration, after which they had all increased at 3 h after administration. The increases in NK and T-helper cell numbers were statistically significant at 3 h after hASC-EV administration (Figure 2b).

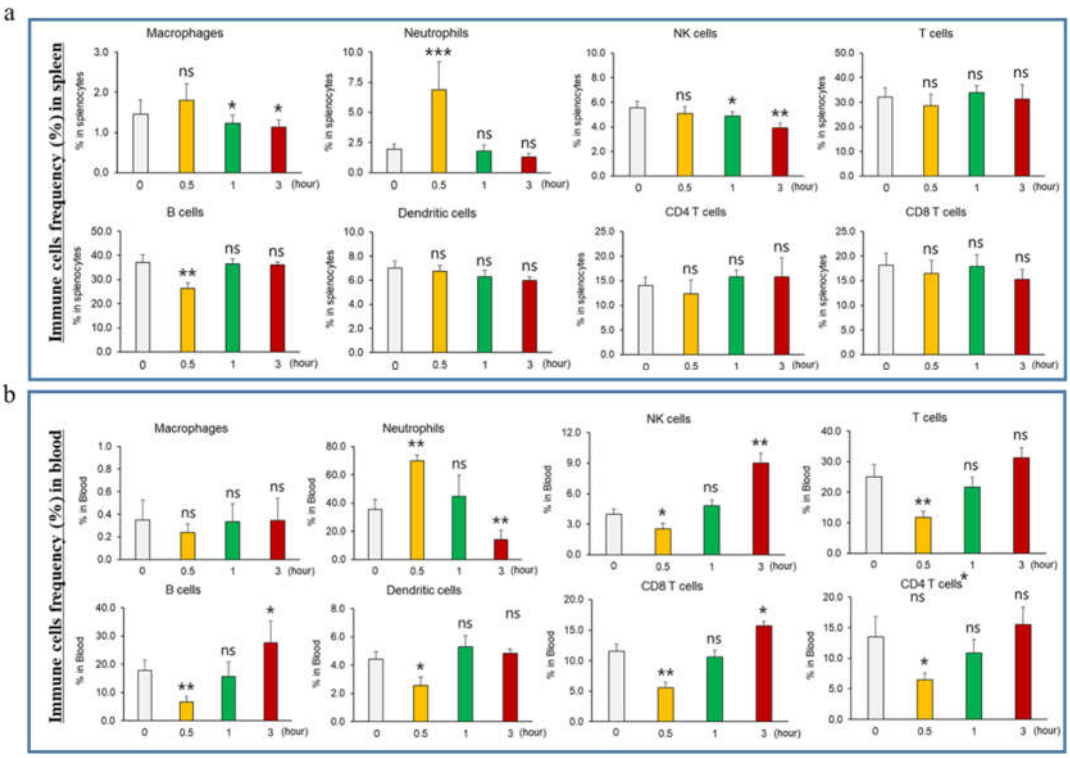

Figure 2. Immune cell-frequency analysis in the spleen and blood of C57BL/6 mice after hASC-EV administration. **(a)** Flow cytometric analysis of macrophages, neutrophils, B cells, and dendritic cells in the spleen using a CytoFLEX flow cytometer. The neutrophil frequency in splenocytes at 0.5 h post treatment is significantly higher (n = 6 mice; one-way ANOVA, ***$p < 0.001$, compared to vehicle control at 0 h). The macrophage frequencies (at 1 and 3 h post treatment) and B cell frequencies (at 0.5 h post treatment) are significantly decreased in the spleen (n = 6 mice; one-way ANOVA, *$p < 0.05$, **$p < 0.01$, compared to the vehicle control at 0 h). **(b)** Flow cytometric analysis of natural killer (NK) and T cells in the spleen. The percentages of NK cells in the spleen at 1 and 3 h post treatment are significantly decreased (n = 6 mice; one-way ANOVA, *$p < 0.05$, **$p < 0.01$, compared to the vehicle control at 0 h). The levels of T cells, including total T cells and cytotoxic ($CD4^+$), and helper ($CD8^+$) T cells, show no significant changes from 0.5 to 3 h after the administration of hASC-EVs. **(c)** Flow cytometric analysis of macrophages, neutrophils, B cells, and dendritic cells in the blood of C57BL/6 mice. The neutrophil frequency in the blood is significantly higher at 0.5 h post treatment but is significantly lower at 3 h post treatment. The macrophage and dendritic cell frequencies at 0.5 h post dosing are decreased significantly. The percentage of B cells in blood is increased significantly at 3 h post dosing (n = 6 mice; one-way ANOVA, *$p < 0.05$, **$p < 0.01$, compared to the vehicle control at 0 h). **(d)** Flow cytometric analysis of natural killer (NK) and T cells in blood samples. The

Preprints (www.preprints.org) | NOT PEER-REVIEWED | Posted: 5 December 2022 doi:10.20944/preprints202212.0069.v1

percentages of NK cells and CD8 T cells in the blood are significantly higher at 3 h post dosing. The percentages of NK cells, T cells, CD8 T cells, and CD4 T cells in the blood are significantly lower at 0.5 h post dosing (n = 6 mice; one-way ANOVA, $*p < 0.05$, $**p < 0.01$, compared to the vehicle control at 0 h).

2.3. Analysis of Immune Cell Frequency in the Spleens and Blood of ICR Mice at Short-term Time Points After Administrating hASC-EVs Five Times

Immune cell frequency in the spleen and blood of ICR mice was analyzed after hASC-EV administration, according to common good laboratory practice (GLP) procedures for nonclinical toxicity tests. This test was performed to compare the immune responses to hASC-EVs in C57BL/6 mice (an inbred mouse strain) as shown in Figures 2. As shown in Figure 3, no significant change was found in immune cells in ICR mouse spleens after hASC-EV administration. Although specific increases or decreases in immune cell frequencies were observed in some mice, individual differences were also observed in the vehicle-control group. Thus, monocytes, macrophages, cytotoxic T cells, T-helper cells, and NK cells did not show any specific changes following hASC-EV administration (Figure 3a). Analyzing the frequencies of immune cells in ICR mouse blood after hASC-EV administration revealed no significant changes in any of the immune cell types investigated (Figure 3b). However, increases in the amount of blood monocytes and macrophages were observed in some mice at 3 h after hASC-EV administration. In addition, the levels of CTL, T-helper, and NK cells decreased at 3 h after administration, but these differences were not significant (Figure 3b). Both flow cytometric and hematological analyses showed that hASC-EV administration affected the increase in the number of monocytes, neutrophils, and macrophages in ICR mice.

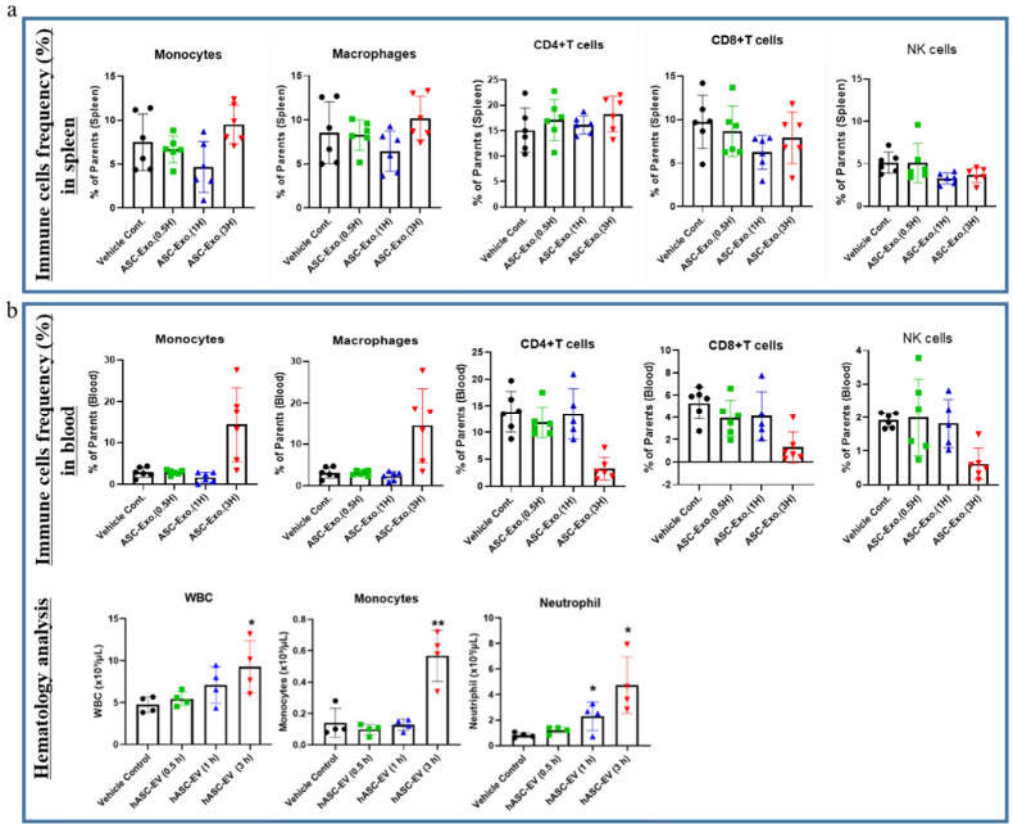

Figure 3. Immune cell frequencies in the spleens and blood of ICR mice. **(a)** Flow cytometric analysis of monocytes, macrophage, cytotoxic ($CD4^+$) and helper ($CD8^+$) T cells and NK cells in ICR mouse spleens based on the mean fluorescence intensity. **(b)** Flow cytometric analysis of monocytes, macrophages, cytotoxic ($CD4^+$) and helper ($CD8^+$) T cells and NK cells in ICR mouse blood. A noticeable increase in blood monocytes and macrophages is observed at 3 h after administration. However, this difference is not statistically significant. No significant change is observed in the

Preprints (www.preprints.org) | NOT PEER-REVIEWED | Posted: 5 December 2022 doi:10.20944/preprints202212.0069.v1

frequencies of cytotoxic ($CD4^+$) and helper ($CD8^+$) T cells in the blood. According to the results of the hematological analysis of white blood cells (WBCs), monocytes, and neutrophils in ICR mouse blood, a significant increase in WBCs, monocytes, and neutrophils were observed at 3 h after administration (n = 5 mice; one-way ANOVA, $*p < 0.05$, $**p < 0.01$, compared to the vehicle control at 0 h).

2.4. Analysis of Immune Cell Frequency in the Spleens of C57BL/6 Mice at 24 h After Administrating hASC-EVs Five Times

To observe the long-term effects of hASC-EVs in C57BL/6 mice, the spleen was harvested at 24 h after the last administration of hASC-EVs. The immune cell frequency in the spleen of C57BL/6 mice was analyzed using flow cytometry. The total number of immune cells was apparently increased in the spleen of the mice treated with the highest dose of hASC-EVs but not significantly (Figure 4b). As shown in Figure 4c, no significant increase in immune cell numbers was found in spleens after hASC-EV administration, except in the positive control group (Figure 4c). The immune cell frequencies in the spleen at 24 h after hASC-EV administration were similar to those observed in the short term after administration. However, hematological analysis was not performed. This analysis will be performed in future.

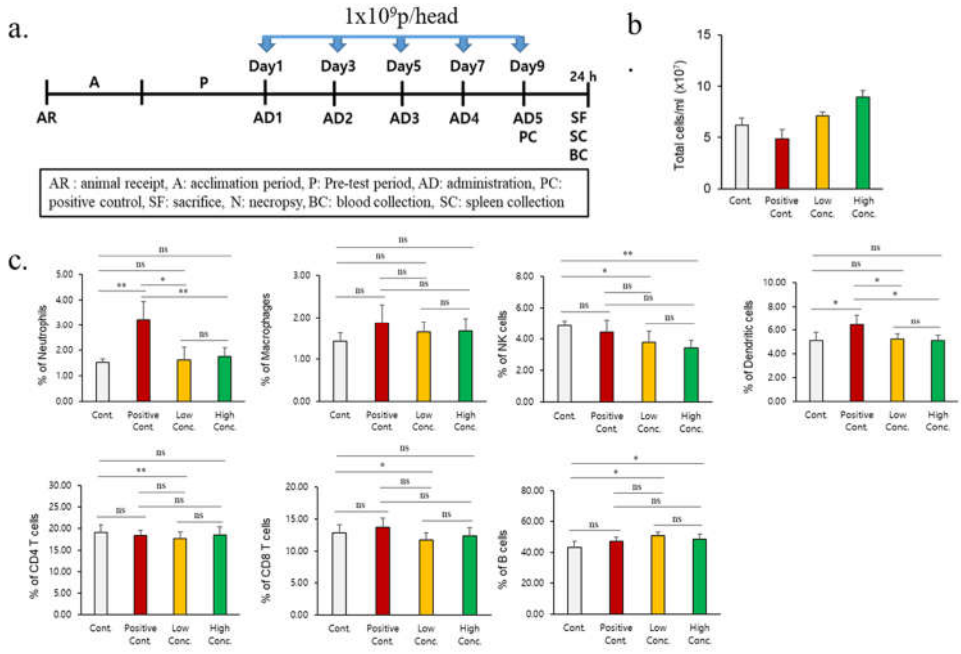

Figure 4. Study design, changes in total cell count, and flow cytometric analysis in the spleens of C57BL/6 after vehicle control, hASC-EV, and positive control administration. **(a)** Experimental schedule for repeated ASC-EV administration in C57BL/6 mice. **(b)** Total cell count in the spleen from each group. No significant changes are observed in all groups. **(c)** Analysis of the frequency of neutrophils, macrophages, NK cells, DC cells, cytotoxic (CD4+) and helper (CD8+) T cells, and B cells in the spleen indicates no significant increase in cell frequency in the hASC-EV-treated group, except in B cell frequency. Neutrophil and dendritic cell frequency is increased significantly in the positive control group.

2.5. Analysis of Immune Cell Frequency in the Spleens of ICR Mice at 24 h After Administering hASC-EVs Five Times

To observe the long-term effects of hASC-EVs in ICR mice, the blood and spleen were harvested at 24 h after the last administration of hASC-EVs. The immune cell frequency in the spleen of ICR mice was analyzed after hASC-EV administration, as described before. As shown in Figure 5a, no significant change was found in immune cells other than NK cells in ICR mouse spleens after hASC-EV administration. However, the percentage of NK cells did not rise considerably (Figure 5a). The increased frequencies of

Preprints (www.preprints.org) | NOT PEER-REVIEWED | Posted: 5 December 2022 doi:10.20944/preprints202212.0069.v1

macrophages, monocytes, and neutrophils were observed in the blood of ICR mice who received the highest dose of hASC-EVs at 3 h after the last administration (Figure 5b). However, the frequency of neutrophil and monocytes in the blood of the mice that received hASC-EV treatment was not increased at 24 h after the last administration (Figure 5b). These results demonstrated that neutrophil and monocyte numbers temporarily increased in hASC-EV-treated mice, then returned to baseline levels over time.

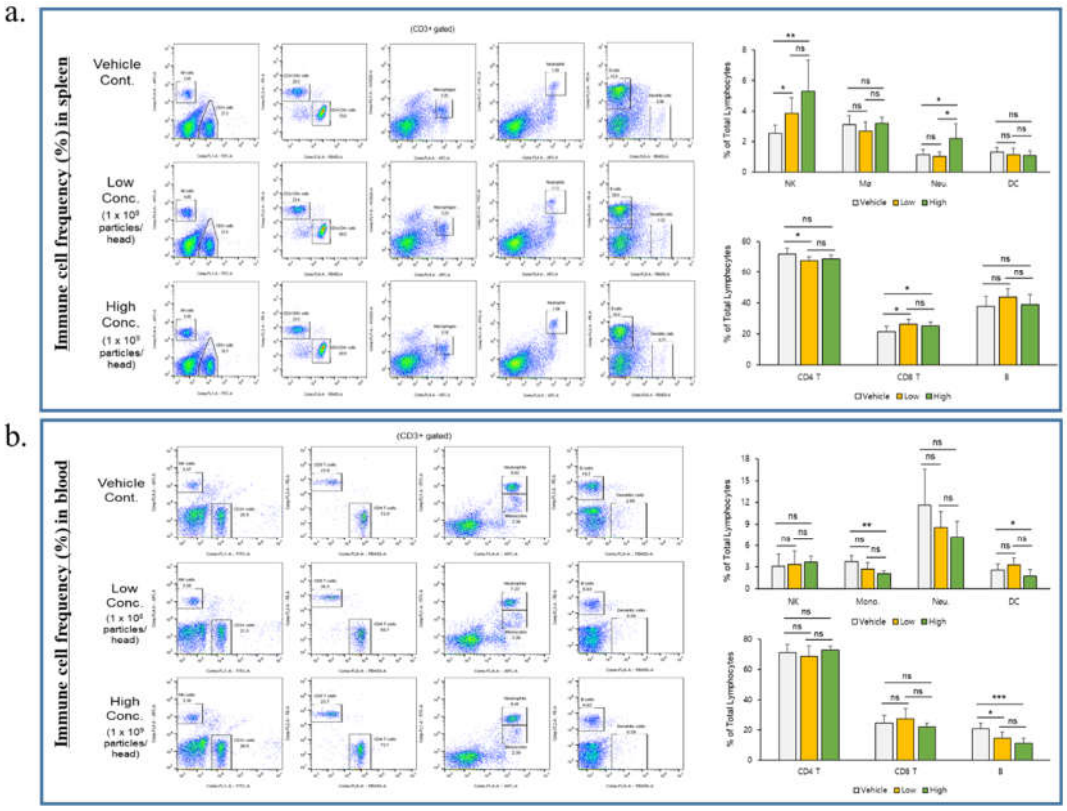

Figure 5. Immune cell frequencies in the spleen and blood of ICR mice. (a) Flow cytometry dot plots. Analysis of monocytes, lymphocytes, neutrophils, and B cells in the blood of ICR mice at 24 h after administering hASC-EVs five times or vehicle control showed that NK cell, neutrophil, and CD8 T cell frequencies increases significantly in the spleens of ICR mice at 24 h after the last administration of hASC-EVs. However, the percentage increases at a very low rate. (b) No specific increase is observed in the immune cell frequency in the blood of ICR mice at 24 h after the last dose (n = 10 mice; one-way ANOVA, $*p < 0.05$, $**p < 0.01$, $***p < 0.001$).

2.6. Immune Cell-Frequency Changes Without Inducing Apoptosis in hPBMCs After hASC-EV Treatment

Apoptosis assay of hPBMCs with Annexin V/7-aminoactinomycin D (7-AAD) after hASC-EV and CPT treatment showed that hASC-EV did not induce apoptosis while CPT induced apoptosis considerably (Figure 6a). Following carboxyfluorescein succinimidyl ester dilution assay using flow cytometry, no considerable changes were observed in the hPBMCs after hASC-EV treatment (Figure 6b). Flow cytometric analysis of B cells among hPBMCs showed that the frequency and activity of monocytes were elevated in hPBMCs treated with phorbol myristate acetate (PMA)/ionomycin, which was used as the positive control in this study. However, no changes in the frequencies of monocytes or B cells were observed in the hASC-EV-treated groups. Although monocytic activities increased along with their frequencies at 6 h after treatment, no changes were observed after 12 or 24 h (Figure 6a–c). Specifically, the abundances of CD86+ cells and activated monocytes increased in a dose-dependent manner in the hASC-EV-treated groups at 6 h after incubation. The middle dose of hASC-EVs was 5 × 108 particles/mL, and the high dose of hASC was 1×10^9 particles/mL. Monocytes activated by hASC-EV administration returned

Preprints (www.preprints.org) | NOT PEER-REVIEWED | Posted: 5 December 2022 doi:10.20944/preprints202212.0069.v1

to normal levels within 12 and 24 h. No significant changes were observed in the frequencies of cytotoxic (CD4+) and helper (CD8+) T cells in hPBMCs. The levels of activated T cells (CD25+ cells) did not increase in the hASC-EV-treated group but increased in the positive control group, during all periods (Figure 6d–f).

Analysis of the effects of hASC-EVs on the frequencies of immune cells in hPBMCs showed that hASC-EVs did not induce robust immune responses, unlike in animals. In other words, hASC-EVs induced some immune responses in animal experiments but showed different patterns between strains and did not induce immune responses in human immune cells. Therefore, when hASC-EVs are used as therapeutic agents in humans, the possibility of an unexpected immune response in the human immune system after administration can be ruled out based on this study.

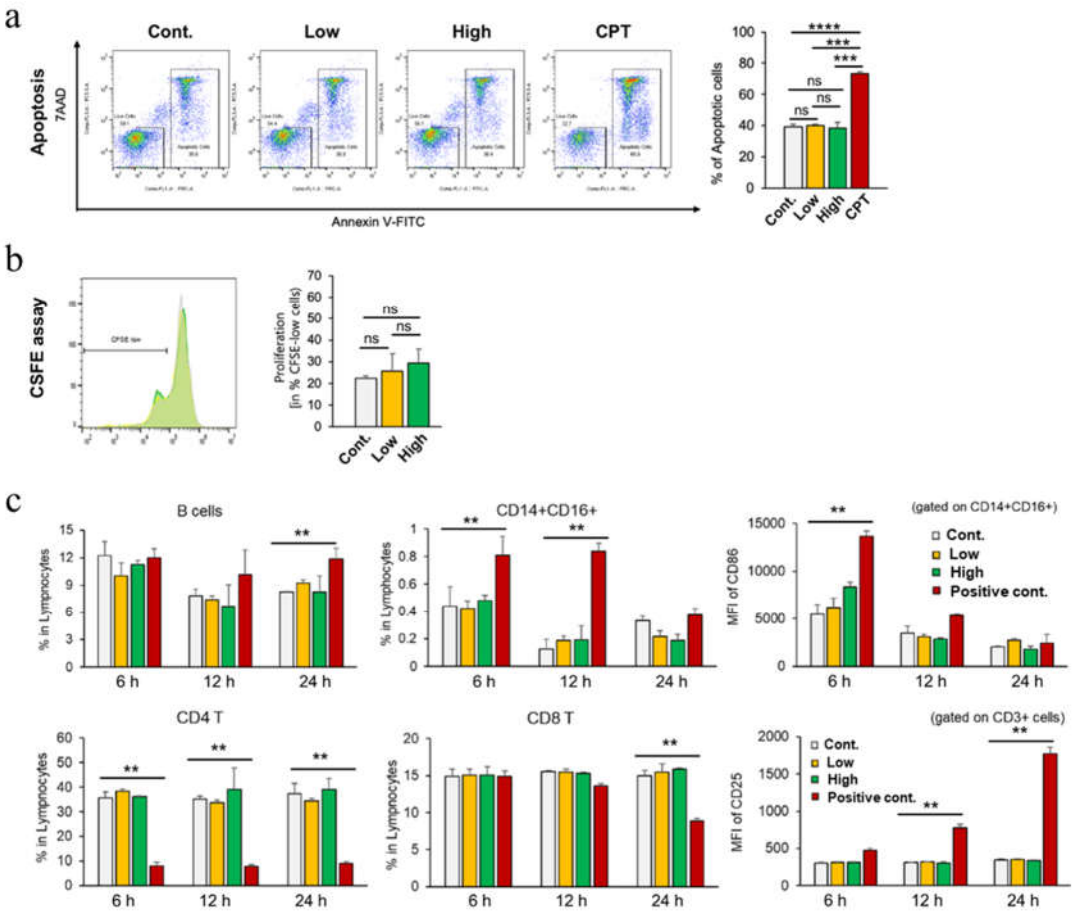

Figure 6. Changes in immune cell frequencies in hPBMCs after hASC-EV treatments. (a) Representative dot plot data (left) and bar graph with error bar (right) generated from Annexin V/7-aminoactinomycin D (7-AAD) assay of hPBMCs treated with control, hASC-EVs, and CPT. (b) Carboxyfluorescein succinimidyl ester dilution assay reveals no considerable changes in hPBMCs upon hASC-EV treatment. (c) Flow cytometric analysis of B cells and cytotoxic (CD4+) and helper (CD8+) T cells in hPBMCs after hASC-EV treatment. The frequency of monocytes is increased after positive control (PMA/ionomycin) treatments but not after hASC-EV treatments. CD86+ cells (activated monocytes) are increased in a dose-dependent manner in the hASC-EV-treated group after 6 h of incubation. The low dose of hASC is 1×10^8 particles/mL, and the high dose of hASC was 1×10^9 particles/mL. However, monocytes are activated by hASC-EV administration returned to their normal levels within 12 h and 24 h. No significant changes in cytotoxic (CD4+) and helper (CD8+) T cell frequencies in hPBMCs are observed. Activated T cells (CD25+ cells) are not increased in the hASC-EV-treated group but are increased in the positive control group during all periods examined. (n = 6; *$p < 0.05$, **$p < 0.01$, ***$p < 0.001$, ****p < 0.0001, Two different tests)3. Discussion.

In this study, we evaluated the effects of hASC-EVs on immune cells in two mouse strains and in hPBMCs *in vitro*. Our data show that the immune responses triggered by

 doi:10.20944/preprints202212.0069.v1

hASC-EVs differ between mouse strains. When hASC-EVs were administered to inbred C57BL/6 mice, the observed immune responses were brief with fast recovery, and the inter-individual differences were small. However, in the out-bred ICR mice, we observed large inter-individual differences in response to hASC-EVs, and the changes in immune cells were more prominent at 3 h post treatment. In addition, the effect of hASC-EVs on human immune cells was weak. Several immune cell types were significantly altered in both mouse strains but were only moderately affected in hPBMCs.

Ample evidence indicated immunotoxicity of EVs in C57BL/6 mice, since this strain is frequently used for preclinical drug efficacy testing and immunological studies [24-26]. In previous reports, the dose of administered EVs ranged from 1 to 250 μg per injection and that the dosing schedule varied from single injection to repeated administration every other day for 3 weeks [27]. EVs derived from HEK293T cells did not induce significant immune responses or toxicity in C57BL/6 mice at the dose levels tested. However, the study group suggested that further immunogenicity or toxicity studies are needed for EVs with other mouse strains or animal species. Therefore, in this study, we analyzed the immune responses to hASC-EVs in C57BL/6 and ICR mice, which are commonly used for immune-related and GLP toxicity studies, respectively. We also examined the immune responses to hASC-EVs in hPBMCs and found that the human immune system is minimally affected by hASC-EVs, in contrast to the mouse immune system. Because we observed no specific immune responses in hPBMCs, ASC-EVs are unlikely to cause fatal side-effects in clinical studies.

EVs contain numerous regulatory proteins, microRNAs, cytokines, and lipids derived from the cells of origin, suggesting their ability to induce an immune response when systemically administered to animals or humans. Regardless of the effectiveness of EVs, their ability to induce an immune response poses a risk for cytokine-release syndrome, which has been a problem in chimeric antigen receptor T cell therapy, which has been used to treat cancer. Therefore, it is essential to study immune responses to hASC-EVs in various animal strains and human cell lines to evaluate their therapeutic potential. Although the frequencies of monocytes, neutrophils, and macrophages characteristically increased at 3 hours, but recovered to levels seen in the control group at 24 h after hASC-EV administration in ICR mice. In this study, we found that the immune responses to hASC-EVs in both mouse strains were slightly different after administration but recovered to a normal range within 24 h. However, when hPBMCs were treated with hASC-EVs, no activation in either cell type was detected at 6, 12 and 24 h. Based on these results, we expect that hASC-EVs will not induce major immune responses in humans.

Biopharmaceuticals such as hASC-EVs are materials derived from human cells, but nonclinical toxicity evaluation is usually performed using rodents such as ICR or C57BL/6 mice or non-rodents such as dogs. However, the conclusion from the results of this study is that hASC-EVs show different immune responses depending on the rodent strain, so it is difficult to predict the immunogenicity when applied to humans. To overcome the limits, we analyzed the direct effect on human immune cells by treating hASC-EVS directly on hPBMCs in this study. Therefore, for the immunotoxicity/ immunogenicity evaluation of biopharmaceuti- cals derived from human cells, it is suggested to utilize human immune cells.

4. Materials and Methods

4.1. Materials

Antibodies against CD11b (BioLegend, San Diego, CA, USA; Cat# 101212, RRID:AB_312795, Cat# 101263, RRID:AB_2629529), CD14 (BioLegend Cat# 367104, RRID:AB_2565888), CD4 (BioLegend Cat# 100443, RRID:AB_2562557, Cat# 357424, RRID:AB_2721519), CD8a (BioLegend Cat# 100737, RRID:AB_10897101), CD8 (BD Biosciences, San Jose, CA, USA; Cat# 563919, RRID:AB_2722546), CD3 (BioLegend Cat# 100210, RRID:AB_389301, Cat# 317318, RRID:AB_1937212), NK1.1 (BioLegend Cat# 108710, RRID:AB_313397), F4/80 (BioLegend Cat# 123135, RRID:AB_2562622), Ly-6G/Ly-

Preprints (www.preprints.org) | NOT PEER-REVIEWED | Posted: 5 December 2022 doi:10.20944/preprints202212.0069.v1

6C (Gr-1) (BioLegend Cat# 108417, RRID:AB_389309), CD45R/B220 (BioLegend Cat# 103207, RRID:AB_312992), CD11c (BioLegend Cat# 117343, RRID:AB_2563099), CD19 (BioLegend Cat# 392508, RRID:AB_2750099), CD25 (BioLegend Cat# 302606, RRID:AB_314276), CD16 (BioLegend Cat# 302012, RRID:AB_314212), CD86 (BioLegend Cat# 105018, RRID:AB_493462, Cat# 305414, RRID:AB_528881), and CD19 (BioLegend Cat# 392508, RRID:AB_2750099) and a Cell Activation Cocktail, which is a mixture of phorbol 12-myristate-13-acetate and ionomycin, were purchased from BioLegend. Enzyme-linked immunosorbent assay (ELISA) kits for determining interferon (IFN)-γ, TNF-α, IL-1β, and IL-6 levels were obtained from R&D Systems (Minneapolis, MN, USA). All mice were purchased from Orient Bio (Seongnam, Republic of Korea).

4.2. hASC-EVs

hASC-EVs were provided by Exostemtech, Inc. (Ansan, Republic of Korea). The detailed characteristics of hASC-EVs and manufacturing steps have been described previously [28,29]. In brief, human adipose-derived stem cells were passaged five times to produce the hASC-EVs. The concentration of hASC-EVs used in this study was 5×10^9 particles/mL, and the mean protein concentration was 212.2 μg/mL. The hASC-EVs were 50–200 nm in diameter and expressed $CD9^+$, $CD63^+$, $CD81^+$, GM130, and calnexin biomarkers [28,29].

4.3. Animal Study Design

All experimental procedures involving animals were approved for use in an American Association for Accreditation of Laboratory Animal Care-accredited safety-evaluation laboratory by the Animal Ethics Committee (our institutional animal care and use committee [IACUC]; approval numbers: 2005-0157 and 2106-0019). Six-week-old male C57BL/6 and ICR mice were acquired 1 week before the start of experiments and acclimatized to the animal facility. All animals were allowed free access to tap water containing lithium, which was filtered through a microfilter and then sterilized with ultraviolet light. To prevent fighting between males, each animal was housed in a single cage. After the acclimatization period was completed, animals were randomly divided into four groups: a vehicle-control group and three hASC-EV-treated groups that were euthanized 0.5, 1, or 3 h after hASC-EV administration. The animals were euthanized at the pre-determined time points. The vehicle-control mice were treated with 1× phosphate-buffered saline (PBS), and 1×10^9 particles were administered to hASC-EV-treated mice five times for 10 days.

4.4. Hematological Analysis

All blood samples were collected after the mice were anesthetized with isoflurane. Blood from the abdominal vena cava was collected into ethylenediaminetetraacetic acid (EDTA)-2K tubes for hematology analysis. White blood cells, monocytes, neutrophils, eosinophils, platelets, reticular red blood cells, and differential counts (leukocytes), were analyzed using the ADVIA2120i Hematology System (Siemens, IL, USA).

4.5. hPBMC Cultures and hASC-EV Treatments for Evaluating Immune Responses

The hPBMCs were purchased from STEMCELL Tech (MA, USA). All cells were provided with documentation confirming that they were mycoplasma-free by securing a Certificate of Analysis. To recover frozen hPBMCs, hPBMCs were thawed in a 37°C water bath 16 h before beginning the experiment and collected by centrifugation at 800 g for 20 min. The collected cells were placed in Roswell Park Memorial Institute (RPMI)-1640 containing 10% fetal bovine serum and incubated at 37°C and 5% CO_2 for 16 h. Then, the hPBMCs were seeded into 48-well plates (Thermo Fisher Scientific, Waltham, MA, USA) at a density of 2×10^5 cells/well (200 μL/well) to test the immune response of a Cell Activation Cocktail (positive control) or hASC-EVs. The median dose of hASC-EVs was 5

 doi:10.20944/preprints202212.0069.v1

× 10^8 particles/mL, and the high dose was 1 × 10^9 particles/mL. The hPBMCs were incubated with the particles for 6, 12, or 24 h.

4.6. Sample Preparation for Flow Cytometry

To analyze the immune cell abundances, a CytoFLEX flow cytometer (Beckman Coulter Life Sciences, Indianapolis, IN, USA) was used. Spleens were dissected and dissociated using a mesh in a Petri dish, transferred to a 15-mL conical tube, and washed with RPMI-1640 (10 mL) containing fetal bovine serum (2%). The obtained samples were centrifuged at 2000 rpm for 10 min at 4°C, with the centrifuge brake set. The supernatant was discarded, the pellet was dislodged from the centrifuge tube, ammonium-chloride-potassium lysing buffer was added, and the pellet was resuspended and lysed at 24 ± 2°C for 3 min. Immune cells isolated from the mouse spleens were aliquoted into fluorescence-activated cell sorting (FACS) tubes at a density of 2.0 × 10^6 cells/tube. After preparing mixtures containing different antibodies and FACS buffer (to analyze different types of immune cells), the cells were dispensed to separate tubes (100 μL/tube) and incubated for 20 min in preparation for FACS analysis. After incubation, FACS buffer was added to each sample tube, the cells were centrifuged and resuspended in FACS buffer, and the cell suspensions were analyzed by flow cytometry.

4.7. ELISA of Plasma Samples

After collecting mouse blood samples in ethylenediaminetetraacetic acid-coated tubes, plasma was separated by centrifugation at 2000 rpm for 15 min. IFN-γ, TNF-α, IL-1β, and IL-6 DuoSet® ELISA Development Systems (R&D Systems) were purchased to analyze for each cytokine, according to the manufacturer's instructions. The analyte-specific antibody (capture antibody) was sprayed onto the plate and incubated at 25°C overnight. On the next day, the capture antibody was washed away with wash buffer. The samples were incubated with appropriate primary antibodies at 25°C for 1 h and then washed three times with the wash buffer. Subsequently, all mouse plasma samples were diluted 2-fold in PBS and transferred to separate wells in the coated ELISA plate. Protein standards (provided by the manufacturer) were added to separate wells to measure the calibration curve. After 1 h of incubation, secondary antibodies (provided by the manufacturer) were applied, and the absorbance values were determined using a SpectraMax iD3 multi-mode microplate reader (Molecular Devices, San Jose, CA, USA).

4.8. Statistical Analysis

GraphPad Prism software was used for statistical analysis of the data generated in this study. One-way analysis of variance (ANOVA) was performed to compare the groups. Statistical results were presented as the mean ± standard deviation. *$p < 0.05$ was considered to reflect a statistically significant difference.

5. Conclusions

The two mouse strains C57BL/6 and ICR showed different immune responses following hASC-EV administration, and hASC-EVs did not induce specific immune responses in hPBMCs. Therefore, we conclude that novel anti-inflammatory therapies can be developed using hASC-EVs, with low risk of inducing specific immune responses in patients.

Supplementary Materials: Figure S1: Monitoring the body temperatures of ICR mice after hASC-EV injections.

Author Contributions: Conceptualization, M.H.Y. and D.O.K.; methodology, M.H.Y, D.O.K and W.K.; formal analysis, M.H.Y. and D.O.K.; investigation, M.H.Y., D.O.K., W.K., Y.C.C., J.S.C. and K.S.L.; resources, Y.C.C., J.S.C. and K.S.L; writing—original draft preparation, M.H.Y.; writing—review and editing, OOO; supervision, Y.W.C. and B.-S.L.; project administration, M.H.Y. and B.-

S.L.; funding acquisition, M.H.Y., J.S.C. and B.S.-L. All authors have read and agreed to the published version of the manuscript.

Funding: This work was supported by grants from the Korean Health Technology R&D Project, Ministry of Health & Welfare (grant number HI20C0437 to M.H.Y.), the Korea Institute of Toxicology, Republic of Korea (grant number 1711159822 to B.-S.L.) and Technological innovation R&D program of MSS (grant number S3032549 to J.S.C.).

Institutional Review Board Statement: The animal study protocol was approved by the Institutional Review Board (or Ethics Committee) of Korea Institute of Toxicology (2005-0157 and 2106-0019).

Informed Consent Statement: Not applicable.
Data Availability Statement: Not applicable

Acknowledgments: we acknowledge Dr. Kyoung-Sik Moon, support given a working space.

Conflicts of Interest: Y.W.C. is a stockholder of Exostemtech, Inc. J.S.C and K.S.L are employed by Exostemtech, Inc. The other authors have no competing interests to declare.

References

1. Amorin, B.; Alegretti, A.P.; Valim, V.; Pezzi, A.; Laureano, A.M.; da Silva, M.A.; Wieck, A.; Silla, L. Mesenchymal stem cell therapy and acute graft-versus-host disease: a review. Hum Cell. 2014, 27, 137–150. DOI: 10.1007/s13577-014-0095-x.
2. Bagno, L.; Hatzistergos, K.E.; Balkan, W.; Hare, J.M. Mesenchymal stem cell-based therapy for cardiovascular disease: progress and challenges. Mol Ther. 2018, 26, 1610–1623. DOI: 10.1016/j.ymthe.2018.05.009.
3. Mukai, T.; Tojo, A.; Nagamura-Inoue, T. Mesenchymal stromal cells as a potential therapeutic for neurological disorders. Regen Ther. 2018, 9, 32–37. DOI: 10.1016/j.reth.2018.08.001.
4. Fernandes, T.L.; Kimura, H.A.; Pinheiro, C.C.G.; Shimomura, K.; Nakamura, N.; Ferreira, J.R.; Gomoll, A.H.; Hernandez, A.J.; Bueno, D.F. Human synovial mesenchymal stem cells good manufacturing practices for articular cartilage regeneration. Tissue Eng Part C Methods. 2018, 24, 709–716. DOI: 10.1089/ten.TEC.2018.0219.
5. Varderidou-Minasian, S.; Lorenowicz, M.J. Mesenchymal stromal/stem cell-derived extracellular vesicles in tissue repair: challenges and opportunities. Theranostics. 2020, 10, 5979–5997. DOI: 10.7150/thno.40122.
6. Becker, A.; Thakur, B.K.; Weiss, J.M.; Kim, H.S.; Peinado, H.; Lyden, D. Extracellular vesicles in cancer: cell-to-cell mediators of metastasis. Cancer Cell. 2016, 30, 836–848. DOI: 10.1016/j.ccell.2016.10.009.
7. Smith, N.C.; Wajnberg, G.; Chacko, S.; Woldemariam, N.T.; Lacroix, J.; Crapoulet, N.; Ayre, D.C.; Lewis, S.M.; Rise, M.L.; Andreassen, R.; Christian, S.L. Characterization of miRNAs in extracellular vesicles released from Atlantic salmon monocyte-like and macrophage-like cells. Front Immunol. 2020, 11, 587931. DOI: 10.3389/fimmu.2020.587931.
8. Robbins, P.D.; Morelli, A.E. Regulation of immune responses by extracellular vesicles. Nat Rev Immunol. 2014, 14, 195–208. DOI: 10.1038/nri3622.
9. Ma, F.; Vayalil, J.; Lee, G.; Wang, Y.; Peng, G. Emerging role of tumor-derived extracellular vesicles in T cell suppression and dysfunction in the tumor microenvironment. J Immunother Cancer. 2021, 9. DOI: 10.1136/jitc-2021-003217.
10. Xu, Z.; Zeng, S.; Gong, Z.; Yan, Y. Exosome-based immunotherapy: a promising approach for cancer treatment. Mol Cancer. 2020, 19, 160. DOI: 10.1186/s12943-020-01278-3.
11. Liu, H.; Liang, Z.; Wang, F.; Zhou, C.; Zheng, X.; Hu, T.; He, X.; Wu, X.; Lan, P. Exosomes from mesenchymal stromal cells reduce murine colonic inflammation via a macrophage-dependent mechanism. JCI Insight. 2019, 4. DOI: 10.1172/jci.insight.131273.
12. Zhao, H.; Shang, Q.; Pan, Z.; Bai, Y.; Li, Z.; Zhang, H.; Zhang, Q.; Guo, C.; Zhang, L.; Wang, Q. Exosomes from adipose-derived stem cells attenuate adipose inflammation and obesity through polarizing M2 macrophages and beiging in White adipose tissue. Diabetes. 2018, 67, 235–247. DOI: 10.2337/db17-0356.
13. Li, Y.; Yun, K.; Mu, R. A review on the biology and properties of adipose tissue macrophages involved in adipose tissue physiological and pathophysiological processes. Lipids Health Dis. 2020, 19, 164. DOI: 10.1186/s12944-020-01342-3.
14. Shigemoto-Kuroda, T.; Oh, J.Y.; Kim, D.K.; Jeong, H.J.; Park, S.Y.; Lee, H.J.; Park, J.W.; Kim, T.W.; An, S.Y.; Prockop, D.J.; Lee, R.H. MSC-derived extracellular vesicles attenuate immune responses in two autoimmune murine models: Type 1 diabetes and uveoretinitis. Stem Cell Rep. 2017, 8, 1214–1225. DOI: 10.1016/j.stemcr.2017.04.008.
15. Su, G.; Ma, X.; Wei, H. Multiple biological roles of extracellular vesicles in lung injury and inflammation microenvironment. BioMed Res Int. 2020, 2020, 5608382. DOI: 10.1155/2020/5608382.
16. Kojima, M.; Costantini, T.W.; Eliceiri, B.P.; Chan, T.W.; Baird, A.; Coimbra, R. Gut epithelial cell-derived exosomes trigger posttrauma immune dysfunction. J Trauma Acute Care Surg. 2018, 84, 257–264. DOI: 10.1097/TA.0000000000001748.
17. Bland, C.L.; Byrne-Hoffman, C.N.; Fernandez, A.; Rellick, S.L.; Deng, W.; Klinke, D.J. Exosomes derived from B16F0 melanoma cells alter the transcriptome of cytotoxic T cells that impacts mitochondrial respiration. FEBS Journal. 2018, 285, 1033–1050. DOI: 10.1111/febs.14396.
18. Du, Y.M.; Zhuansun, Y.X.; Chen, R.; Lin, L.; Lin, Y.; Li, J.G. Mesenchymal stem cell exosomes promote immunosuppression of regulatory T cells in asthma. Exp Cell Res. 2018, 363, 114–120. DOI: 10.1016/j.yexcr.2017.12.021.

19. Abd Elmageed, Z.Y.; Yang, Y.; Thomas, R.; Ranjan, M.; Mondal, D.; Moroz, K.; Fang, Z.; Rezk, B.M.; Moparty, K.; Sikka, S.C.; Sartor, O.; Abdel-Mageed, A.B. Neoplastic reprogramming of patient-derived adipose stem cells by prostate cancer cell-associated exosomes. Stem Cells. 2014, 32, 983–997. DOI: 10.1002/stem.1619.
20. Antonyak, M.A.; Li, B.; Boroughs, L.K.; Johnson, J.L.; Druso, J.E.; Bryant, K.L.; Holowka, D.A.; Cerione, R.A. Cancer cell-derived microvesicles induce transformation by transferring tissue transglutaminase and fibronectin to recipient cells. Proc Natl Acad Sci U S A. 2011, 108, 4852–4857. DOI: 10.1073/pnas.1017667108.
21. Melo, S.A.; Sugimoto, H.; O'Connell, J.T.; Kato, N.; Villanueva, A.; Vidal, A.; Qiu, L.; Vitkin, E.; Perelman, L.T.; Melo, C.A.; Lucci, A.; Ivan, C.; Calin, G.A.; Kalluri, R. Cancer exosomes perform cell-independent microRNA biogenesis and promote tumorigenesis. Cancer Cell. 2014, 26, 707–721. DOI: 10.1016/j.ccell.2014.09.005.
22. Zhu, X.; Badawi, M.; Pomeroy, S.; Sutaria, D.S.; Xie, Z.; Baek, A.; Jiang, J.; Elgamal, O.A.; Mo, X.; Perle, K.; Chalmers, J.; Schmittgen, T.D.; Phelps, M.A. Comprehensive toxicity and immunogenicity studies reveal minimal effects in mice following sustained dosing of extracellular vesicles derived from HEK293T cells. J Extracell Vesicles. 2017, 6, 1324730. DOI: 10.1080/20013078.2017.1324730.
23. Yüksel, M.; Laukens, D.; Heindryckx, F.; Van Vlierberghe, H.; Geerts, A.; Wong, F.S.; Wen, L.; Colle, I. Hepatitis mouse models: from acute-to-chronic autoimmune hepatitis. Int J Exp Pathol. 2014, 95, 309–320. DOI: 10.1111/iep.12090.
24. Scattoni, M.L.; Crawley, J.; Ricceri, L. Ultrasonic vocalizations: a tool for behavioural phenotyping of mouse models of neurodevelopmental disorders. Neurosci Biobehav Rev. 2009, 33, 508–515. DOI: 10.1016/j.neubiorev.2008.08.003.
25. Alvarez-Erviti, L.; Seow, Y.; Yin, H.; Betts, C.; Lakhal, S.; Wood, M.J. Delivery of siRNA to the mouse brain by systemic injection of targeted exosomes. Nat Biotechnol. 2011, 29, 341–345. DOI: 10.1038/nbt.1807.
26. Yang, Z.; Xie, J.; Zhu, J.; Kang, C.; Chiang, C.; Wang, X.; Wang, X.; Kuang, T.; Chen, F.; Chen, Z.; Zhang, A.; Yu, B.; Lee, R.J.; Teng, L.; Lee, L.J. Functional exosome-mimic for delivery of siRNA to cancer: in vitro and in vivo evaluation. J Control Release. 2016, 243, 160–171. DOI: 10.1016/j.jconrel.2016.10.008.
27. Geiger, A.; Walker, A.; Nissen, E. Human fibrocyte-derived exosomes accelerate wound healing in genetically diabetic mice. Biochem Biophys Res Commun. 2015, 467, 303–309. DOI: 10.1016/j.bbrc.2015.09.166.
28. Woo, C.H.; Kim, H.K.; Jung, G.Y.; Jung, Y.J.; Lee, K.S.; Yun, Y.E.; Han, J.; Lee, J.; Kim, W.S.; Choi, J.S.; Yang, S.; Park, J.H.; Jo, D.G.; Cho, Y.W. Small extracellular vesicles from human adipose-derived stem cells attenuate cartilage degeneration. J Extracell Vesicles. 2020, 9, 1735249. DOI: 10.1080/20013078.2020.1735249.
29. Lee, K.S.; Lee, J.; Kim, H.K.; Yeom, S.H.; Woo, C.H.; Jung, Y.J.; Yun, Y.E.; Park, S.Y.; Han, J.; Kim, E.; Sul, J.H.; Jung, J.M.; Park, J.H.; Choi, J.S.; Cho, Y.W.; Jo, D.G. Extracellular vesicles from adipose tissue-derived stem cells alleviate osteoporosis through osteoprotegerin and miR-21-5p. J Extracell Vesicles. 2021, 10, e12152. DOI: 10.1002/jev2.12152.